Computation of trailing edge noise from an incompressible flow calculation

By Assad A. Oberai† AND M. Wang

A new methodology for calculating low Mach number trailing edge noise is developed and tested. The input to this methodology is the fluctuating surface pressure obtained from an incompressible, turbulent flow calculation. The surface pressure is used to calculate an intermediate incident pressure. This pressure in conjunction with the sound-hard boundary condition yields the scattered pressure which accounts for the effect of the rigid airfoil. Through numerical experiments it is found that the proposed methodology is sensitive to noise in the data. Modifications that circumvent this sensitivity are under consideration.

1. Introduction

The purpose of this study is to compute noise generated by turbulent flow over a lifting surface. It is well known that if the Mach number is small then such problems can be solved using Lighthill's acoustic analogy (see Lighthill (1954)) as a starting point. In the frequency domain, Lighthill's analogy requires the solution of the Helmholtz equation to obtain a correction to the pressure. In the near field, this "correction" contains both hydrodynamic and acoustic components of pressure, whereas in the far field, it reduces to the acoustic pressure.

In particular, we wish to extend and apply the formulation developed in Oberai & Hughes (2000). In that study, the authors split pressure into an incident part and a scattered part. The incident field contains noise generated by fluid flow in the absence of the airfoil. The scattered field accounts for the effect of the rigid airfoil and is determined by applying the sound hard condition on the surface of the airfoil. This approach is akin to the works of Crighton & Leppington (1971), Chandiramani (1973), Chase (1971) and Howe (1998), among others. The distinguishing feature of the approach used in Oberai & Hughes (2000) and incorporated in our formulation is the numerical computation of the scattered field. This allows us to account for the effect of the geometry of the airfoil accurately, in particular, to model the effect of the finite chord on pressure directivity and scaling.

The work done in Oberai & Hughes (2000) was based on the vortex sound theory and was applied to the case where noise sources in the fluid were idealized as frozen vortices that are convected past the airfoil. In this study we consider the development of this methodology in the context of Lighthill's acoustic analogy and apply it to the case where the sources are determined from an incompressible, turbulent calculation. The calculation we have used for this purpose is the large-eddy simulation of turbulent flow over a wedge. The details of this calculation are provided in Wang & Moin (2000).

The layout of this manuscript is as follows: In Section 2, we develop the methodology

† Division of Mechanics and Computation, Stanford University

to compute noise in a general setting. In Section 3, we describe the specific steps involved in applying this methodology to our problem. In Section 4, we present numerical results, and we end with conclusions in Section 5.

2. Derivation of the methodology

We begin with time-harmonic version of Lighthill's analogy for a given non-dimensional frequency ω. This equation is valid in the fluid domain Ω_f, exterior to a rigid structure denoted by Ω_s, with a wet boundary denoted by Γ_s.

$$-\nabla^2\tilde{p} - k^2\tilde{p} = \nabla\cdot(\nabla\cdot\tilde{\mathbf{T}}) \quad \text{in } \Omega_f \tag{2.1}$$

$$\nabla\tilde{p}\cdot\mathbf{n} = 0 \quad \text{on } \Gamma_s \tag{2.2}$$

$$\lim_{r\to\infty} r(\tilde{p}_{,r} - ik\tilde{p}) = 0 \tag{2.3}$$

In the above equations, p denotes pressure-like variable that reduces to the acoustic pressure in the far-field, $k = \omega M$ is the wavenumber, $M = U/C_0$ is the Mach number, where U is the free-stream velocity, and C_0 is the speed of sound in the undisturbed ambient medium. The sign $\tilde{}$ over a quantity indicates its Fourier transform in time. In solving (2.1) through (2.3), it is assumed that Lighthill's turbulence tensor $\mathbf{T}$ is known. For our case, $\mathbf{T}$ is determined by solving the incompressible, Navier-Stokes equations and is given by:

$$T_{ij} = u_i u_j \tag{2.4}$$

where u_i is the fluid velocity in the ith direction. Equation (2.2) is the sound hard condition applied on the surface of the airfoil denoted by Γ_s. Equation (2.3) is the Sommerfeld condition that requires all waves to be outgoing at infinity. Throughout this paper all variables are assumed to be non-dimensional. Spatial coordinates $\mathbf{x}$ are non-dimensionalized by L, a suitably chosen length parameter. Time t is non-dimensionalized by U/L. Density ρ is non-dimensionalized by ρ_∞, its reference value in the undisturbed ambient fluid. Pressure is non-dimensionalized by the quantity $\rho_\infty U^2$.

Following the development in Oberai & Hughes (2000), we split the pressure p in the above equation into an "incident" part denoted by p_I and a "scattered" part denoted by p_S. The incident part is determined by replacing the rigid airfoil by the undisturbed ambient fluid. The equations that determine p_I are:

$$-\nabla^2\tilde{p}_I - k^2\tilde{p}_I = \nabla\cdot(\nabla\cdot\tilde{\mathbf{T}}) \quad \text{in } \Omega_f \bigcup \Omega_s \tag{2.5}$$

$$\lim_{r\to\infty} r(\tilde{p}_{I,r} - ik\tilde{p}_I) = 0 \tag{2.6}$$

The equations for the scattered part of the pressure may be determined by subtracting the equations for the incident pressure from the equations for the total pressure. These are given by

$$-\nabla^2\tilde{p}_S - k^2\tilde{p}_S = 0 \quad \text{in } \Omega_f \tag{2.7}$$

$$\nabla\tilde{p}_S\cdot\mathbf{n} = -\nabla\tilde{p}_I\cdot\mathbf{n} \quad \text{on } \Gamma_s \tag{2.8}$$

$$\lim_{r\to\infty} r(\tilde{p}_{S,r} - ik\tilde{p}_S) = 0 \tag{2.9}$$

Note that the equations for the scattered pressure are driven only by the normal derivative of the incident pressure on Γ_s and do not involve any variables from the fluid calculation.

It is well known that for the trailing-edge problem the incident pressure which represents the noise generated by quadrupoles in free space contributes very little to the far-field noise. In fact, it has been established that (see Crighton & Leppington (1971) for example),

$$|\tilde{p}_I| = \begin{cases} |\tilde{p}_S| \times O(M) & \lambda \gg l \\ |\tilde{p}_S| \times O(M^{1/2}) & \lambda \ll l \end{cases} \tag{2.10}$$

where λ is the acoustic wavelength and l is the chord length of the airfoil. Thus for small M, the contribution from the incident pressure may be neglected. In that case, we require the incident pressure only on the surface of the airfoil to calculate the scattered pressure. For the case when the acoustic sources are less than a fraction of a wavelength away from the trailing-edge, we may treat the calculation of the incident pressure to be incompressible. This amounts to setting $k = 0$ in (2.5) and (2.6). This approximation allows us to express the incident pressure in terms of the the surface pressure p_f obtained from the incompressible flow calculation. This derivation is described in the following paragraph.

Let $G(\mathbf{x}, \mathbf{y})$ be the free space Green's function for the Laplacian in three dimensions. Then for $k = 0$ in (2.5) we have,

$$p_I(\mathbf{x}) = -\int_{\Omega_f \bigcup \Omega_s} G(\mathbf{x}, \mathbf{y})\ \nabla \cdot (\nabla \cdot \mathbf{T}(\mathbf{y}))\ d\Omega \tag{2.11}$$

$$= -\int_{\Omega_f} G(\mathbf{x}, \mathbf{y})\ \nabla \cdot (\nabla \cdot \mathbf{T}(\mathbf{y}))\ d\Omega \tag{2.12}$$

$$= \int_{\Omega_f} G(\mathbf{x}, \mathbf{y})\ \nabla^2_{\mathbf{y}}\ p_f(\mathbf{y})\ d\Omega \tag{2.13}$$

$$= \int_{\Omega_f} \nabla^2_{\mathbf{y}}\ G(\mathbf{x}, \mathbf{y})\ p_f(\mathbf{y})\ d\Omega$$

$$+ \int_{\Gamma_s} \Big(- G(\mathbf{x}, \mathbf{y})_{,n_y}\ p_f(\mathbf{y}) + G(\mathbf{x}, \mathbf{y})\ p_{f,n}(\mathbf{y}) \Big)\ d\Gamma \tag{2.14}$$

$$= p_f(\mathbf{x}) + \int_{\Gamma_s} \Big(- G(\mathbf{x}, \mathbf{y})_{,n_y}\ p_f(\mathbf{y}) + Re^{-1} G(\mathbf{x}, \mathbf{y}) u_{n\ ,nn} \Big)\ d\Gamma \tag{2.15}$$

$$\approx p_f(\mathbf{x}) - \int_{\Gamma_s} G(\mathbf{x}, \mathbf{y})_{,n_y}\ p_f(\mathbf{y})\ d\Gamma \tag{2.16}$$

To arrive at (2.13) from (2.12) In the above derivation, we have made use of the pressure-Poisson equation satisfied by the fluid pressure p_f in an incompressible calculation. To arrive at (2.14) from (2.13), we have used Green's formula (see Courant & Hilbert(1989) page 252.) To arrive at (2.15) from (2.14), we have made use of the fact that $p_{f,n} = Re^{-1} u_{n\ ,nn}$, on the surface of the airfoil. This expression can be derived from momentum equation in the wall normal direction and the continuity equation. Finally, to arrive at (2.16), we have assumed that Re is sufficiently large such that the second term in the surface integral in (2.15) may be neglected.

Taking the normal derivative of the incident pressure in (2.16),taking the limit when $\mathbf{x}$ approaches the surface of the airfoil, and making use of the fact that $\tilde{p}_{f,n}$ may be neglected once again, we arrive at the following convenient expression for the normal

FIGURE 1. Cross-sectional view of the model airfoil.

derivative of the incident pressure:

$$\nabla p_I(\mathbf{x}) \cdot \mathbf{n} = -\int_{\Gamma_s} G(\mathbf{x},\mathbf{y})_{,n_x\ n_y}\ p_f(\mathbf{y})\ d\Gamma \tag{2.17}$$

Equation (2.17) in conjunction with Eqs. (2.7)-(2.9) defines a complete set of equations that need to be solved to determine the far-field acoustic pressure. It is noteworthy that the only input to these equations from the fluid calculation is the knowledge of the surface pressure.

3. Implementation of the proposed methodology

The methodology derived in the previous section involves two steps. The first is the calculation of the normal derivative of the incident pressure using (2.17), and the second is the calculation of the scattered field, obtained by solving (2.7) through (2.9). In this section we describe how these calculations are performed.

3.1. *Calculation of the incident pressure*

The cross-sectional view of the model airfoil is shown in Fig. 1. In the figure and the following development, subscript 1 denotes the stream-wise direction, subscript 3 denotes the span-wise direction, and subscript 2 denotes the direction normal to the flat portion of the upper surface of the wedge. The surface of the wedge is denoted by Γ_s. Since the airfoil is assumed to be infinite in the span-wise extent in the flow calculation, we have $\Gamma_s = \bar{\Gamma}_s \times (-\infty, \infty)$, where $\bar{\Gamma}_s$ is a curve in the $y_3 = 0$ plane. The free-space Green's function for the Laplacian in three dimensions denoted by G is given by:

$$G(\mathbf{x},\mathbf{y}) = \frac{1}{4\pi}\frac{1}{|\mathbf{x}-\mathbf{y}|} \tag{3.1}$$

The calculation of the normal derivative of the incident pressure on Γ_s involves using (3.1) in (2.17) and evaluating the surface integral for each point $\mathbf{x}$. This calculation can be simplified if we take into account the fact that all variables in the fluid calculation, including the surface pressure, can be expressed as:

$$\begin{aligned}\tilde{p}_f(y_1,y_2,y_3) &= \sum_{j=-N/2+1}^{N/2} \hat{p}_f(y_1,y_2) e^{i(2\pi j/L_z)y_3} \\ &= \sum_{k_3} \hat{p}_f e^{ik_3 y_3}\end{aligned} \tag{3.2}$$

where L_z is the size of the computational domain in the span-wise direction.

Using (3.1) and (3.2) in (2.17) we arrive at

$$\tilde{p}_{I,n} = \sum_{k_3} \frac{1}{4\pi} \int_{\bar{\Gamma}} \int_{-\infty}^{\infty} \left(\frac{3}{r^5} f_1 - \frac{1}{r^3} f_2\right) \hat{p}_f\ e^{ik_3 y_3}\ dy_3\ dy_1 dy_2$$

$$= \sum_{k_3} \frac{1}{4\pi} \int_{\bar{\Gamma}} \hat{p}_f \Big(f_1 \int_{-\infty}^{\infty} \frac{3e^{ik_3 y_3}}{r^5} dy_3 - f_2 \int_{-\infty}^{\infty} \frac{e^{ik_3 y_3}}{r^3} dy_3 \Big) dy_1 dy_2 \tag{3.3}$$

where

$$r^2 = (x_1 - y_1)^2 + (x_2 - y_2)^2 + (x_3 - y_3)^2 \tag{3.4}$$

$$f_1 = (x_1 - y_1)(x_1 - y_1) n_{x_1} n_{y_1} + (x_1 - y_1)(x_2 - y_2) n_{x_1} n_{y_2} + (x_2 - y_2)(x_1 - y_1) n_{x_2} n_{y_1} + (x_2 - y_2)(x_2 - y_2) n_{x_2} n_{y_2} \tag{3.5}$$

$$f_2 = n_{x_1} n_{y_1} + n_{x_2} n_{y_2} \tag{3.6}$$

Now letting

$$\bar{r}^2 = (x_1 - y_1)^2 + (x_2 - y_2)^2 \ , \ \bar{y}_3 = y_3 - x_3 \tag{3.7}$$

in (3.3) we have

$$\tilde{p}_{I,n} = \sum_{k_3} \hat{p}_{I,n} e^{ik_3 y_3} \tag{3.8}$$

$$\hat{p}_{I,n} = \frac{1}{2\pi} \int_{\bar{\Gamma}} \hat{p}_f \left(\frac{3f_1}{2} \int_{-\infty}^{\infty} \frac{e^{ik_3 \bar{y}_3}}{(\bar{r}^2 + \bar{y}_3^2)^{5/2}} d\bar{y}_3 - \frac{f_2}{2} \int_{-\infty}^{\infty} \frac{e^{ik_3 \bar{y}_3}}{(\bar{r}^2 + \bar{y}_3^2)^{3/2}} d\bar{y}_3 \right) dy_1 dy_2 \tag{3.9}$$

Evaluating the integral in the $\bar{y}_3$ direction (see Gradshteyn & Ryzhik(1994)) we get

$$\hat{p}_{I,n} = \frac{1}{2\pi} \begin{cases} \displaystyle\int_{\bar{\Gamma}} \hat{p}_f \left(f_1 |k_3|^2 K_2(|k_3|\bar{r}) - \frac{f_2}{r} |k_3| K_1(|k_3|\bar{r}) \right) dy_1 dy_2 & k_3 \neq 0 \\ \displaystyle\int_{\bar{\Gamma}} \frac{\hat{p}_f}{\bar{r}^2} \Big(2f_1 - f_2 \Big) dy_1 dy_2, & k_3 = 0 \end{cases} \tag{3.10}$$

where $K_n(z)$ is the modified Bessel function of order n (see Abramowitz & Stegun (1970), pg. 374). Equations (3.10) and (3.8) are the expressions used to evaluate the normal derivative of the pressure field. Through the use of a Fourier transform in the y_3 direction, we have transformed the surface integral in (2.17) to a line integral for each k_3 in (3.10).

3.2. *Evaluation of the scattered field*

Once the incident field is known, it remains to solve Eqs. (2.7) through (2.9) to determine the scattered field. To solve these equations we write an equivalent weak formulation for the problem, given by: Find $\tilde{p}_S \in \mathcal{S} = H^1(\Omega_a)$, such that

$$(\nabla w, \nabla \tilde{p}_S) - k^2 (w, \tilde{p}_S) - (w, M(\tilde{p}_S))_{\Gamma_a} = -(w, \nabla \tilde{p}_I \cdot \mathbf{n})_{\Gamma_s}, \forall w \in \mathcal{S} \tag{3.11}$$

In the above equation the inner product $(\cdot, \cdot)$ is defined as

$$(w, u) \equiv \int_{\Omega_a} w^* u d\omega \tag{3.12}$$

where Ω_a is the bounded domain obtained by truncating the unbounded fluid domain Ω_f at the surface Γ_a. The Euler-Lagrange equations associated with (3.11) are the Helmholtz equation (2.7), the boundary condition on Γ_s (2.8), and the following boundary condition on Γ_a

$$\nabla \tilde{p}_S \cdot \mathbf{n} = M(\tilde{p}_S) \tag{3.13}$$

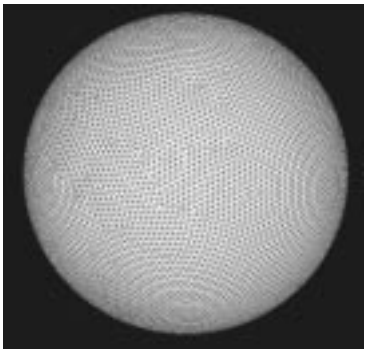

FIGURE 2. Finite element mesh on the truncating surface.

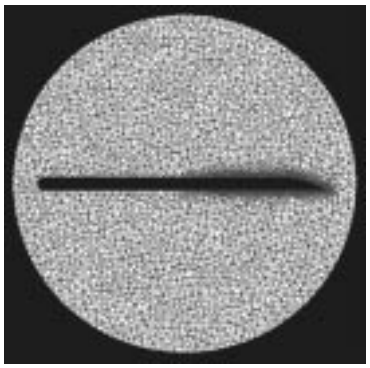

FIGURE 3. Finite element mesh through the mid-span.

In this example we choose Γ_a to be a sphere and M to be the exact Dirichlet to Neumann (DtN) map (see Grote & Keller (1995)) that renders (3.11) equivalent to (2.7) through (2.9). We solve (3.11) using a Galerkin approximation and the finite element discretization.

4. Numerical results and discussion

The time-history of surface pressure obtained from the fluid calculation was split into 8 windows of equal length (see Wang & Moin (2000) for details on the fluid calculation). Data for each of these windows was then Fourier transformed in time to obtain the surface pressure distribution for each frequency ω. Each of these sets were further Fourier transformed in the y_3 direction, and (3.10) was used to evaluate the contribution of each mode (k_3) to the incident pressure. The contribution from all of the modes was then summed using using an inverse Fourier transform (3.8) to obtain $\tilde{p}_{I,n}$.

To calculate the scattered pressure field, (3.11) was solved using a Galerkin approximation and finite element discretization. The truncating boundary for the acoustic calculation denoted by Γ_a was chosen to be a sphere of radius 12.5 units. On this surface the truncated modified DtN map (Grote & Keller (1995)) was applied. The acoustic domain completely encloses the wedge whose chord length is 21.5 units. The details of the geometry of the wedge are described in Wang & Moin (2000). For the acoustic calculation the span-wise length of the wedge was chosen to be 4 units. The incident surface pressure was applied on a strip of width $L_z = 0.5$ units in the span-wise direction, centered along the mid-span of the wedge. In the LES calculation only the part of the wedge 8 units upstream from the trailing edge was modeled. Thus surface pressure data was available for only this portion. To account for this in the acoustic calculation, starting from a location 4.5 units upstream of the trailing edge, $\tilde{p}_{I,n}$ was linearly scaled down to zero at 8 units from the trailing edge.

The resulting linear system of equations was solved using the QMR algorithm in conjunction with the SSOR preconditioner, with the special matrix-vector product algorithms described in Oberai, Malhotra, & Pinsky (1998). We employed 761,017 tetrahedral finite elements to model the acoustic domain. This corresponds to 147,036 unknowns. The surface mesh on the truncating surface is shown in Fig. 2, and the finite element mesh though the mid-plane of the wedge is shown in 3. In this figure we observe the clustering of the mesh near the surface of the airfoil to resolve the incident pressure field.

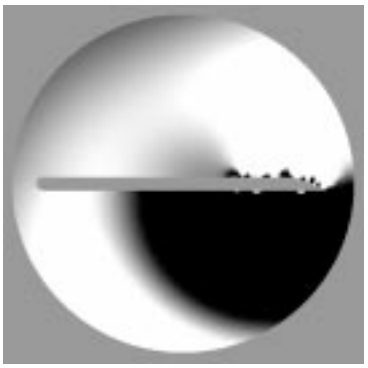

FIGURE 4. Real part of the solution for $\omega = 3.376$.

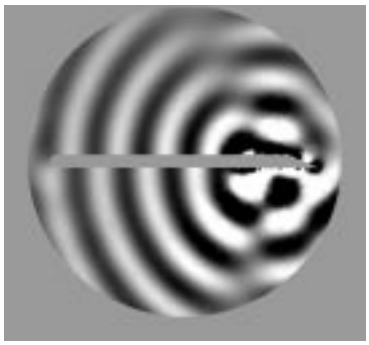

FIGURE 5. Real part of the solution for $\omega = 20.28$.

The problem of trailing edge noise shows an interesting behavior with the variation of the ratio of the acoustic wavelength to the chord length (λ/l.) In the low frequency regime $\lambda/l \gg 1$, the far-field pressure directivity is like that of a dipole, and the scaling of *non-dimensional* pressure (non-dimensionalized by $\rho_\infty U^2$) intensity with the Mach number is of order M^2. In the high frequency regime, $\lambda/l \ll 1$, the far-field pressure directivity is like that of a cardioid, and the scaling of pressure intensity is of order M^1. In Oberai & Hughes (2000), using an approach analogous to the one developed herein, the authors were able to recover these two theoretical extremes and also shed light on the intermediate range of frequencies. However, in that study the authors modeled the noise sources as idealized line vortices and derived an analytical expression for the incident pressure field for the acoustic calculation. It is one of the goals of this study to validate the applicability of this approach for the case when the flow field and hence the noise sources are obtained from a LES of turbulent flow. Through extensive numerical tests we have found the numerical noise in the data from the turbulent calculation is sufficient to corrupt the behavior of the solution substantially, and the approach described above may lead to erroneous results. We base our conclusion on the unphysical far-field directivity pattern obtained for some test cases and, more quantitatively, on the incorrect scaling of pressure intensity with Mach number obtained for most test cases.

First, we present results for a fixed Mach number ($M = 0.088$) at two frequencies ($\omega = 3.376\&20.28$.) The real part of the solution for these cases is shown in Figs. 4 and 5, and the imaginary parts of the solution are shown in Figs. 6 and 7. The corresponding far-field directivity patterns are shown in Figs. 8 and 9. While these pictures appear reasonable, at least qualitatively, it is difficult to draw any definitive conclusions from them.

To assess whether the proposed approach captures the characteristics of the trailing edge problem, we examine the variation of total far-field acoustic intensity $\tilde{\phi}$ with the Mach number. We define the total acoustic intensity as

$$\tilde{\phi} = \lim_{R\to\infty} \int_{\Gamma_R} |\tilde{p}_S|^2 \, d\Gamma \tag{4.1}$$

It can be easily verified that this quantity tends to a constant value in the limit $R \to \infty$ and that in the low frequency regime $\lambda \gg l$ it varies with Mach number as $\tilde{\phi} = O(M^2)$, while in the high frequency regime $\lambda \ll l$ it varies as $\tilde{\phi} = O(M^1)$. In Fig. 10, for a given frequency $\omega = 10.14$, we have plotted $\tilde{\phi}$ as a function of Mach number. In this

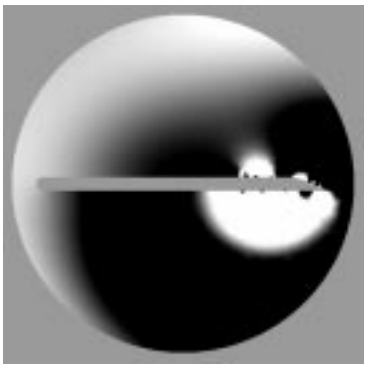

FIGURE 6. Imaginary part of the solution for $\omega = 3.376$.

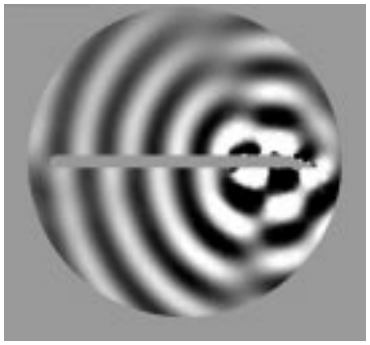

FIGURE 7. Imaginary part of the solution for $\omega = 20.28$.

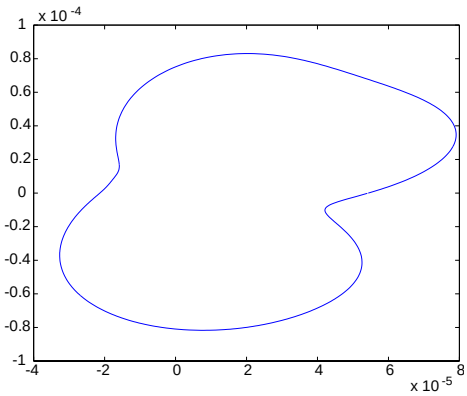

FIGURE 8. Far-field pressure directivity for $\omega = 3.376$.

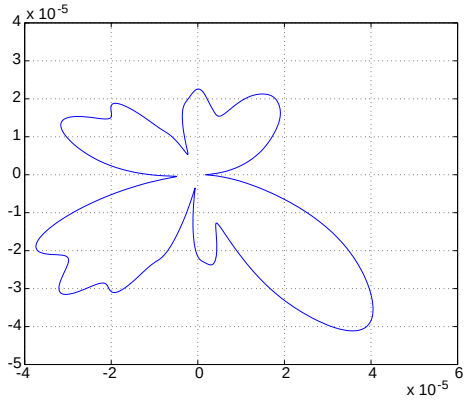

FIGURE 9. Far-field pressure directivity for $\omega = 20.28$.

plot $M \in (0.026, 0.158)$, which corresponds to $l/\lambda \in (0.89, 5.3)$. In this regime we would expect $\tilde{\phi} = O(M^1)$, associated with a cardioid-like directivity. However, from the plot we observe that $\tilde{\phi} = O(M^0)$, which is the scaling for a monopole source. This indicates the inability of the proposed approach to solve the problem accurately.

This shortcoming can be understood analytically by applying the proposed approach to a simplified problem. Consider the noise produced by a distribution of quadrupole sources above a rigid infinite plate. Let the position of the plate be given by $y_2 = 0$. The solution to this problem is the sum of the noise produced in free space by the quadrupoles above the plate and the noise produced by a fictitious distribution obtained by mirroring the original sources about $y_2 = 0$. It can be easily shown (see Goldstein (1976)) that for compact acoustic sources $L \ll \lambda$, the intensity of noise scales as $O(M^4)$. To solve this problem using the approach developed in this paper, we would first calculate the incident pressure $\tilde{p}_{I,n}$ associated with the given distribution of quadrupoles. Thereafter, we would calculate the scattered field given by:

$$\tilde{p}_S(\mathbf{x}) = \int_{\Gamma_s} G_S(\mathbf{x}, \mathbf{y})\, \tilde{p}_{I,n}(\mathbf{y}) d\Gamma \tag{4.2}$$

In the above integral G_S is the sound-hard Green's function. For the infinite plate, using

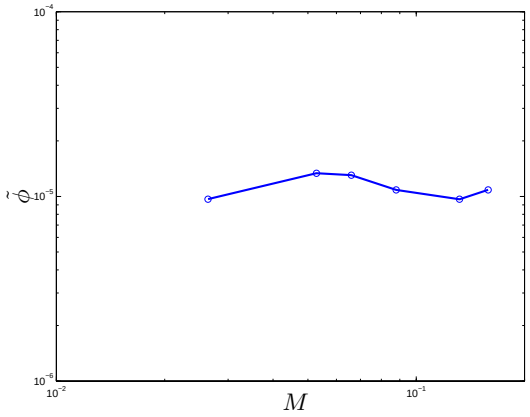

FIGURE 10. Total far-field acoustic intensity $\tilde{\phi}$ as a function of Mach number M, for $\omega = 10.14$.

the method of images, this is given by

$$G_S(\mathbf{x},\mathbf{y}) = \frac{1}{4\pi}\Big(\frac{e^{ik|\mathbf{x}-\mathbf{y}|}}{|\mathbf{x}-\mathbf{y}|} + \frac{e^{ik|\mathbf{x}-\mathbf{y}'|}}{|\mathbf{x}-\mathbf{y}'|}\Big) \tag{4.3}$$

where $\mathbf{y}' \equiv [y_1, -y_2, y_3]^T$. Using this expression in (4.2) and evaluating the integral for an observation point in the far-field and a compact acoustic source around the origin, we get:

$$\begin{aligned}\tilde{p}_S(\mathbf{x}) &\approx \frac{1}{2\pi}\frac{e^{ik|\mathbf{x}|}}{|\mathbf{x}|} \times \int_{\Gamma_s} \tilde{p}_{I,n}(\mathbf{y}) d\Gamma \\ &\approx O(M^0) \times \int_{\Gamma_s} \tilde{p}_{I,n}(\mathbf{y}) d\Gamma \end{aligned} \tag{4.4}$$

For this result to have the correct behavior with Mach number (i.e. $O(M^4)$), the integral in (4.4) must behave as $O(M^4)$. For acoustic sources obtained from an incompressible flow calculation, $\tilde{p}_{I,n}$ has no Mach number dependence, and the best case scenario is given by the case when the integral in the above equation vanishes. For turbulent flow calculations it is unreasonable to expect that $\tilde{p}_{I,n}$ can be determined with sufficient accuracy for this to happen. Therefore, we can expect the proposed formulation to yield results consistent with the presence of spurious monopoles while the true solution precludes their possibility. This is precisely what is observed in Fig. 9.

5. Conclusions

We have developed and implemented a formulation to calculate noise generated by low-Mach number flows. The advantages of this approach are that in the acoustic problem it accounts for the geometry of the structure accurately and requires only the surface pressure from an incompressible fluid calculation. We have applied this methodology to compute the noise generated by a turbulent flow over a trailing edge. We have found that this approach is not robust enough to provide accurate results with pressure data obtained from turbulent calculations. This is attributed to the fact that in calculating the scattered field, all sources are treated as monopole sources. Therefore, to accurately predict noise that has higher-order multipole components, the incident pressure needs to

be evaluated extremely accurately so that cancellations may lead to the right acoustic component. For the problem solved in this study, we have found that this is not the case.

To overcome this drawback it seems natural to work with an approach that takes as input sources of the highest multipole order in the solution (quadrupoles for our case.) One such approach is to solve the weak form of Lighthill's equations (2.1) through (2.3). This has been done in Oberai, Roknaldin & Hughes (2000), where the authors were able to reproduce the dipole character of the acoustic solution for the low frequency case. As a continuation of this study, we will explore the applicability of this approach to our problem.

REFERENCES

Abramowitz, M. & Stegun, I. A. 1970 Handbook of Mathematical Functions. Dover Publications Inc.

Chandiramni, K. L. 1973 Diffraction of evanescent waves, with applications to aerodynamically scattered sound and radiation from unbaffled plates. *J. Acoust. Soc. Am.* **55(1)**, 18-29.

Chase, D. M. 1986 Sound Radiated by Turbulent Flow off a Rigid Half-Plane Obtained from a Wavevector Spectrum of Hydrodynamic Pressure. *J. Acoust. Soc. Am.* **52(3)**, 1011-1023.

Courant R. & Hilbert D. 1989 *Methods of Mathematical Physics*. John Wiley & Sons.

Crighton, D. G. & Leppington, F. G. 1970. On the scattering of aerodynamic noise. *J. Fluid Mech.* **46(3)**, 577-597.

Goldstein M. E. 1976 *Aeroacoustics*. McGraw-Hill, Inc.

Gradshteyn, I. S. & Ryzhik, I. M. 1994 *Table of integrals, series, and products*. Academic Press.

Grote, M. J. & Keller, J. B. 1995 On non-reflecting boundary conditions. *J. Comput. Phys.* **122(2)**, 231-243.

Howe, M. S. 1998 Trailing Edge Noise at Low Mach Numbers. *J. Sound Vib.* **225(2)**, 211-238.

Lighthill, M. J. 1954 On Sound Generated Aerodynamically I. General Theory. *Proc. Roy. Soc. (London).* **211A, 1107**, 1-32.

Oberai, A. A. & Hughes, T. J. R. 2000 Computation of trailing-edge noise for a finite chord airfoil. *In preparation.*

Oberai A. A., Malhotra, M. and Pinsky, P. M. 1995 Implementation of the Dirichlet-to-Neumann radiation condition for iterative solution of the Helmholtz equation. *App. Num. Math.* **27(4)**, 443-464.

Oberai, A. A., Roknaldin, F. & Hughes, T. J. R. 2000 Computational Procedures for Determining Structural Acoustic Response due to Hydrodynamic Sources. To appear in *Comp. Meth. Appl. Mech. & Engr.*

Wang, M., & Moin, P. 2000 Computation of trailing-edge flow and noise using large-eddy simulation. To appear in *AIAA J.*